

Aggregation-governed oriented growth of inorganic crystals at an organic template

Sumit Kewalramani, Geoffrey Dommett, Kyungil Kim, Guennadi Evmenenko, Haiding Mo, Benjamin Stripe, and Pulak Dutta

Department of Physics and Astronomy, Northwestern University, Evanston, Illinois 60208

(Received 15 August 2006; accepted 28 November 2006; published online 14 December 2006)

X-ray studies performed during the growth of CdCO_3 and MnCO_3 crystals from supersaturated aqueous solutions, at fatty acid monolayer templates, reveal that the nucleates are nearly three-dimensional powders below a threshold supersaturation. However, at higher supersaturations, the crystals are preferentially oriented with the $\{0\ 1\ 2\}$ direction vertical. Scanning electron microscope images of samples transferred to substrates show discrete crystals at low concentrations, while at higher concentrations the crystals self-aggregate to form linear chains and sheets. The authors speculate that preferential alignment at the organic-inorganic interface is enhanced as a consequence of oriented aggregation of crystals. The role of monolayer-ion interactions in governing the morphologies and the resulting orientation of the inorganic nucleate is discussed. © 2006 American Institute of Physics. [DOI: [10.1063/1.2424937](https://doi.org/10.1063/1.2424937)]

I. INTRODUCTION

Inorganic nucleation at organic templates mimics biomineralization. It is believed that in such processes, the form and orientation of inorganic crystals at the organic-inorganic interface are determined by the arrangement and the chemical functionality of the organic molecules.¹ Monomolecular layers of insoluble surfactants floating over supersaturated aqueous subphases are widely used for studying nucleation and crystal growth at ordered organic surfaces. The two-dimensional arrangement of organic headgroups can be systematically modified by the application of lateral surface pressure or temperature, and the surface charge by varying the subphase pH.² Such tunable Langmuir monolayers have been used to grow oriented crystals of CaCO_3 ,³ PbS and CdS ,⁴ $\text{CaC}_2\text{O}_4 \cdot \text{H}_2\text{O}$,⁵ BaSO_4 ,⁶ BaF_2 ,⁷ SrF_2 ,⁷ $2\text{PbCO}_3 \cdot \text{Pb}(\text{OH})_2$,⁸ etc. Oriented crystalline growth under Langmuir monolayers has been shown to stem from molecular recognition, i.e., a stereochemical or a geometric match at the organic-inorganic interface.¹

However, recent studies suggest another possibility: crystal aggregation based self-assembly mechanisms can also lead to oriented growth at templates. For example, Banfield *et al.*⁹ find that iron oxyhydroxide crystallites in natural biomineralization orient at the periphery of organic matrix via formation of nanoparticle chains and sheets. Similarly, calcite crystals grown in polyacrylamide hydrogel networks aggregate to form single crystalline clusters with a pseudo-octahedral morphology,¹⁰ and the authors also suggest that aggregation is a general feature of crystallization at high supersaturation. However, the influence of organic matrix in determining the orientation and morphology of the nucleated crystals has not been investigated in these bulk studies.

We have grown cadmium and manganese carbonate crystals from highly supersaturated subphases under fatty acid Langmuir monolayers, and characterized the growth process with *in situ* grazing incidence x-ray diffraction (GID)

and *ex situ* scanning electron microscopy (SEM). We find that, above a critical supersaturation, preferentially oriented crystalline growth is enhanced by spontaneous self-aggregation of crystallites. SEM studies are also used to compare the morphology of crystals grown under fatty acid and alcohol monolayers and in the absence of the monolayer.

II. EXPERIMENT

Supersaturated subphases of cadmium carbonate and manganese carbonate [the solubility of both metal carbonates are $\sim 10^{-3}$ mM/l (Refs. 11 and 12)] were prepared by mixing equal volumes of aqueous solutions of cadmium chloride and manganese chloride, respectively, with sodium bicarbonate in a 1:2 concentration ratio. The concentrations used were CdCl_2 : 0.2 and 0.4 mM at 10 °C and MnCl_2 : 1.25, 2.5, and 10 mM at 20 °C. The pH for cadmium carbonate solutions was adjusted to 8 with sodium hydroxide and was left unadjusted for manganese carbonate solutions [measured to be 7.5 ± 0.2 (1.25 mM), 7.35 ± 0.2 (2.5 mM), and 7.20 ± 0.2 (10 mM)]. Monolayers of heneicosanoic acid ($\text{C}_{20}\text{H}_{41}\text{COOH}$) were spread over supersaturated subphases and were compressed by a mechanical barrier, in a Langmuir trough, until the surface pressure rose slightly above 0 dyn/cm. This ensures that the monolayer is all in a single condensed phase rather than a coexistence of gas phase and a condensed phase. The samples were exposed to a beam of synchrotron x rays with $\lambda = 1.5498$ Å in the GID geometry. The x-ray beam was focused vertically ~ 600 μm and horizontally ~ 1 cm. Crossed soller slits in front of the detector defined a horizontal resolution $K_{XY} \sim 0.01$ Å⁻¹ and a vertical resolution $K_Z \sim 0.05$ Å⁻¹. Other details of the GID setup can be found in Ref. 13. As Langmuir monolayers are powders in the horizontal plane, the in-plane momentum transfer vector K_{XY} cannot be decomposed into x and y components. However, the vertical component K_Z can be measured separately.

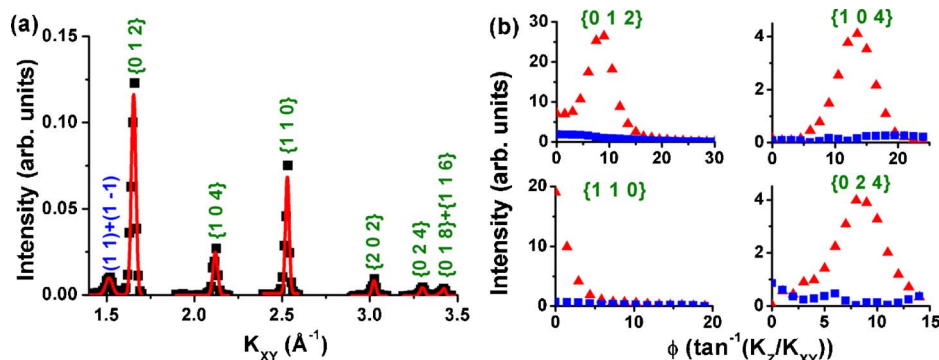


FIG. 1. Cadmium carbonate nucleation under a fatty acid Langmuir monolayer: (a) Typical in-plane diffraction scan of interfacial cadmium carbonate. All allowed strong peaks are visible (labeled with curly brackets). The degenerate peak closest to origin is a monolayer peak. (b) “Debye” ring scans for inorganic peaks. At low cadmium ion concentration in the subphase (■, 0.2 mM), the uniform intensity distribution in ring scans indicates an absence of preferred crystallographic orientation. At higher cadmium ion concentration (▲, 0.4 mM), cadmium carbonate nucleate is preferentially oriented with $\{0\ 1\ 2\}$ crystal face parallel to the water surface.

To investigate the influence of different functional groups on the morphology of the grown crystals, nucleation experiments were also performed in the presence of heneicosanol ($C_{21}H_{43}OH$) monolayers and in the absence of an organic template. Samples were prepared in a Langmuir trough as described above or alternatively in petri dishes, by spreading appropriate quantities of monolayer material (calculated from limiting area/organic molecule obtained from current and previous GID studies¹⁴) over supersaturated cadmium and manganese carbonate subphases.

Samples for *ex situ* morphology analysis were obtained by vertically dipping cleaned silicon wafers through the film surface, such that the crystals were transferred by surface tension. X-ray diffraction experiments were performed on the transferred inorganic films, using a four-circle Huber diffractometer, to confirm that the orientation of crystals grown under fatty acid monolayer is preserved upon transfer onto solid substrates. An FEI Nova Nano 600 SEM was used for morphology characterization. Because of the insulating nature of the transferred inorganic crystals, SEM imaging was performed in the low vacuum mode with water vapor. The acceleration voltages used varied between 3 and 9 kV.

III. RESULTS AND DISCUSSION

The cadmium and manganese carbonate species nucleated in our experiments are trigonal synthetic otavite and rhodochrosite [$CdCO_3$ and $MnCO_3$; space group: $R\text{-}3C$ (167)], which can alternatively be described by hexagonal unit cells. We shall use hexagonal unit cell notation throughout the paper. The observed lattice parameters for the cadmium carbonate lattice are $a_{Cd}=4.95\text{ \AA}$ and $c_{Cd}=16.32\text{ \AA}$ and are slightly larger than the known bulk values; $a=4.93\text{ \AA}$ and $c=16.31\text{ \AA}$.¹⁵ Similarly, the observed lattice parameters for manganese carbonate $a_{Mn}=4.82\text{ \AA}$ and $c_{Mn}=15.75\text{ \AA}$ are expanded compared to the known bulk values of $a_b=4.77\text{ \AA}$ and $c_b=15.64\text{ \AA}$.¹⁶ Previous studies of calcite ($CaCO_3$), an isomorphic carbonate with similar lattice spacings, have shown that crystals grown in the presence of sodium ions have expanded unit cells.¹⁷ However, studies of crystal growth of calcite under Langmuir monolayers clearly demonstrate that incorporation of sodium ions in the crystal

lattice has no effect on the morphology and orientation of the nucleate.¹⁸ Crystal morphologies in our experiment as well as are solely determined by the template monolayer. On the other hand, our *in situ* GID studies show that the subphase supersaturation has a profound effect on the degree of crystal alignment at the organic-inorganic interface.

A. Grazing incidence x-ray diffraction results

GID scans performed during crystal growth show that at low metal ion concentrations (0.2 mM for $CdCO_3$ and 1.25 mM for $MnCO_3$), the nucleated carbonate crystallites do not have a noticeable preferred crystallographic orientation. As expected from three dimensional (3D) powders, all the allowed strong peaks are visible in a horizontal radial scan [Figs. 1(a) and 2(a)]. The diffraction maxima move along “Debye” rings rather than the “Bragg rods” (data not shown) and the intensity distribution along these rings, in the experimentally accessible reciprocal space, is quite uniform.

At higher supersaturations, the peak positions still follow the “Debye” rings. However, the intensity distribution along the rings is not uniform. Instead, the intensity distribution is peaked at different positions for crystal planes with different indices. The rocking curves for four strong cadmium carbonate and two strong manganese carbonate peaks are presented in Figs. 1(b) and 2(b), respectively. The position of these peaks indicates that the nucleated crystals are preferentially oriented close to $\{0\ 1\ 2\}$ crystallographic planes parallel to plane of monolayer substrate.¹⁹

Enhanced preferred orientation, with increased supersaturation, is also reflected in the inversion of relative intensities of $\{1\ 1\ 0\}$ and $\{1\ 0\ 4\}$ peaks in the in-plane scans. For, 3D powder samples of these carbonates the $\{1\ 0\ 4\}$ peaks have the highest intensity.^{15,16} However, when the crystals are preferentially aligned with $\{0\ k\ l\}$ crystallographic plane parallel to the water surface, $\{1\ 1\ 0\}$ is an in-plane peak while $\{1\ 0\ 4\}$ is not. Therefore, the ratio of the observed intensities $I\{1\ 1\ 0\}/I\{1\ 0\ 4\}$, in a radial scan through $K_z=0$, increases with improved average orientation of the nucleate.

The ratios of intensities of the two peaks, $I\{1\ 1\ 0\}/I\{1\ 0\ 4\}$, calculated after accounting for Lorentz-polarization and scattering area corrections,²⁰ are ~ 0.9 and

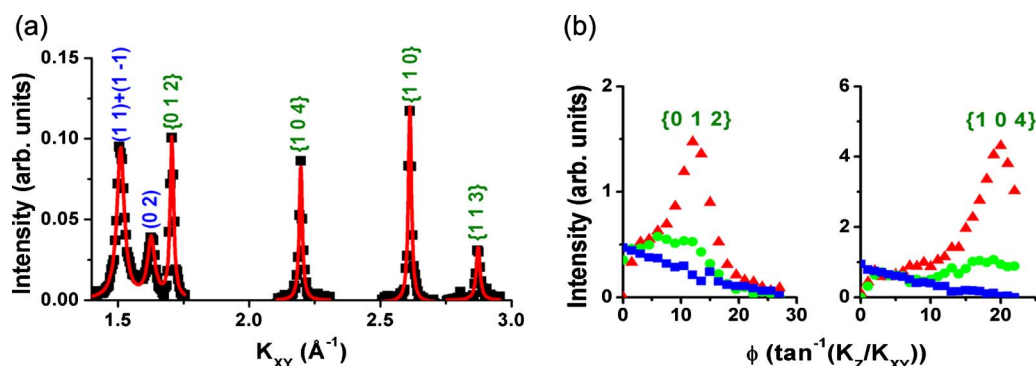


FIG. 2. Manganese carbonate nucleation under a fatty acid Langmuir monolayer: (a) typical in-plane diffraction scan of interfacial rhodochrosite. All allowed strong peaks are visible (labeled with curly brackets). The peaks closest to origin are monolayer peaks. (b) “Debye” ring scans for inorganic peaks. At low manganese ion concentration in the subphase (■, 1.25 mM), the uniform intensity distribution in ring scans indicates an absence of preferred crystallographic orientation. At higher manganese ion concentration (●, 2.5 mM and ▲, 10 mM), manganese carbonate nucleate is preferentially oriented with $\{0\ 1\ 2\}$ crystal face parallel to the water surface.

0.4 for cadmium carbonate and manganese carbonate, respectively, at the lowest supersaturations studied and increase to ~ 8 for CdCO_3 and ~ 3.2 for MnCO_3 , at the highest concentrations. It should be noted that even at the lowest concentrations the ratio of intensities are higher than the predicted two dimensional powder values of 0.36 and 0.19. This suggests that the crystals have a preferred orientation plane even at low supersaturation. The only possible explanation for “flat” ring scans at these concentrations is that the degree of misorientation is $\geq 28^\circ$ full width at half maximum (FWHM), beyond the maximum accessible range of our apparatus. This is consistent with our observations for manganese carbonate that the degree of misorientation decreases with increased supersaturation. Lorentzian fits to the ring scans reveal the degree of misorientation to be $\sim 14^\circ$ FWHM at 2.5 mM and $\sim 9^\circ$ at 10 mM.

B. Molecular recognition at template-mineral interface

The $\{0\ 1\ 2\}$ crystallographic direction consists of alternating layers of metal ions and tilted carbonate ions (the carbonate plane normal is aligned with the hexagonal c axis). We shall show that simple considerations of geometric and stereochemical matches, at the organic-inorganic interface, are insufficient descriptions for the relative stabilization of this face.

Before proceeding further, it is worthwhile to review our knowledge of the nucleation of another isomorphous mineral, calcite, under fatty acid monolayers. Isomorphous calcium carbonate grown under untilted phases of fatty acid monolayers has been reported to nucleate with the neutral $\{1\ 0\ 0\}$ crystal face parallel to the template surface.²¹ In this orientation, the arrangement of carbonate ions mimics the carboxylate headgroup geometry at the interface. Further, the surface lattice of hexagonally packed fatty acid monolayers ($a_o \sim 5\ \text{\AA}$ and $b_o \sim 8.6\ \text{\AA}$) matches closely the $\{1\ 0\ 0\}$ rectangular plane of calcite ($a_{ca} \sim 5\ \text{\AA}$ and $b_{ca} \sim 8.5\ \text{\AA}$). Thus an epitaxial match mechanism can easily explain the alignment of $\{1\ 0\ 0\}$ crystal face with the template surface.

A similar match should be possible, especially for the CdCO_3 $\{1\ 0\ 0\}$ face ($a_{100} = 4.95\ \text{\AA}$ and $b_{100} = 8.16\ \text{\AA}$), via a small ($< 4\%$) compression of the “soft” organic template.

However, the crystal orientation observed in the case of cadmium and manganese carbonates is $\{0\ 1\ 2\}$. A geometric match between the organic and inorganic $\{0\ 1\ 2\}$ surface lattices can be found in the case of cadmium and manganese carbonates also, but the shared supercells found are quite large and not as simple as the one proposed above (details are in Ref. 22). Further, the arrangement of carbonate ions along $\{0\ 1\ 2\}$ direction can replicate the arrangement of carboxylate headgroups only if the monolayer molecules are tilted with respect to the interface normal. Rod scans at the monolayer peak positions (data not shown), performed during crystal growth of CdCO_3 and MnCO_3 , clearly show that the monolayers are in untilted phases. For untilted carboxylate molecules, the condition of stereochemical match would only be met by $\{hk0\}$ crystallographic planes. The stabilization of $\{0\ 1\ 2\}$ orientation over $\{1\ 0\ 0\}$ orientation demonstrates that simple geometric considerations alone are inadequate in explaining the face selection in matrix-templated crystal growth.

We suggest that the nature of ion-organic headgroup interactions plays a significant role in governing the orientation of the grown crystals. The distinct nature of interactions between Ca, Cd, and Mn ions with the fatty acid headgroups can explain the relative stabilization of different crystal faces at the template surface.

The binding constants for Ca^{2+} —carboxylate headgroups are low and it is questionable if a plane containing only Ca^{2+} ions can be stabilized under fatty acid monolayers.²³ In contrast, Mn^{2+} and Cd^{2+} ions or their hydrated ionic complexes interact strongly with fatty acid headgroups. In fact, the presence of these ions even in dilute quantities is known to induce the formation of thin inorganic superstructures at the organic-inorganic interface.²⁴ Neither the nature of these interactions nor the form in which these ions interact with carboxylate headgroups is known. These results, however, suggest that planes containing only cadmium or manganese ions can be stabilized under fatty acid monolayers. Our morphological studies performed on crystals grown under different monolayers (next subsection) further highlight the role of ion-headgroup interactions.

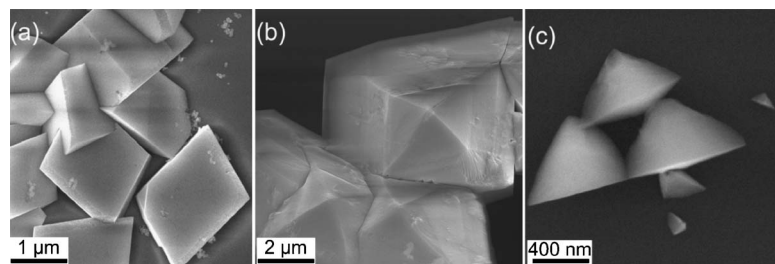


FIG. 3. Predominant morphologies of cadmium carbonate crystals grown (a) in the absence of an organic template, (b) under alcohol monolayers, and (c) under fatty acid monolayers.

C. Scanning electron microscopy results

Samples for SEM studies were obtained by dipping cleaned silicon wafers through the film interface. Morphological studies were performed on crystals grown under fatty acid and alcohol monolayers and in the absence of any organic template (Figs. 3 and 4). Cadmium carbonate crystals grown in the absence of a monolayer consist of randomly oriented intergrown $\{1\ 0\ 4\}$ rhombohedra [Fig. 3(a)]. Crystals grown under neutral heneicosanol monolayers also consist of $\{1\ 0\ 4\}$ rhombs, however, with a central elevated feature [Fig. 3(b)]. This morphology has been previously observed in the crystal growth of calcite under fatty acid monolayers.²⁵ The morphology of cadmium carbonate crystals grown under fatty acid monolayers is supersaturation independent, and the crystals have rounded edges and faces [Fig. 3(c)]. Since GID studies have clearly demonstrated that these crystals grow preferentially oriented with $\{0\ 1\ 2\}$ direction vertical, we expect the morphology to be closely related to the typical $\{0\ 1\ 2\}$ tetrahedral morphology.^{26,27}

The three faces in the tetrahedron are the neutral $\{1\ 0\ 4\}$ crystallographic faces and the basal isosceles triangular face is a $\{0\ 1\ 2\}$ type crystal face. The $(0\ 1\ 2)$ triangular face consists of edges parallel to the $\langle 1\ 0\ 0 \rangle$, $\langle 4\ 2\ -1 \rangle$ and $\langle 2\ -2\ 1 \rangle$ crystallographic directions with the largest angle in the triangle being 77.1° . For many crystals observed in our experiments, the angles formed by the intersection of tangents drawn through the center of rounded edges match the expected values very closely. These observations clearly show that the basal face is indeed a $\{0\ 1\ 2\}$ type crystallographic face.

For MnCO_3 crystals grown under fatty acid monolayers, the morphology is different from the typical tetrahedral crystals described above [Fig. 4(d)]. We have not identified all the crystallographic faces. Since GID studies indicate that the crystals are preferentially oriented with $\{0\ 1\ 2\}$ face parallel to the substrate, we assume that the basal planes are $\{0\ 1\ 2\}$ type. In contrast, under heneicosanol monolayers $(0\ 0\ 1)$ and $\{1\ 0\ 4\}$ faces are expressed [Fig. 4(c)]. The top face is the $(0\ 0\ 1)$ crystallographic face and the side step faces are $\{1\ 0\ 4\}$

$4\}$ type faces. The angle between $(0\ 0\ 1)$ crystallographic face and $(1\ 0\ 4)$ face is 43.3° . When the crystals are viewed at a tilt of $\sim 45^\circ$, the angles between the edges of the side faces closely match the expected values, 76.9° and 103.1° , for the $\{1\ 0\ 4\}$ rhombohedra.

Similarly, in the absence of monolayer $\{1\ 0\ 4\}$ rhomb is the predominant crystal type [Fig. 4(a)]. However, a few crystals ($\sim 5\%$) also nucleate with the top face $(0\ 0\ 1)$ [Fig. 4(b)]. Thus, for both MnCO_3 and CdCO_3 , crystal morphologies and hence the orientation at the organic-inorganic interface are determined by monolayer type.

Since the monolayers influence the crystal face selection, it is surprising that the degree of misorientation at low supersaturations is so high. Previous GID studies of crystal growth of barium and strontium fluoride, under fatty acid monolayers, show that while the alignment of crystals at the template surface is perfect during the earliest growth phases, the crystals become misoriented during latter growth stages.⁷

Cadmium carbonate and manganese carbonate are sparingly soluble minerals. In solutions where solubility is low the solution remains metastable below a critical supersaturation, whereas above the critical supersaturation the nucleation rate turns catastrophic.²⁸ Thus, it is possible that we may not have observed the earliest growth stages, where the crystals may have been well aligned at the interface.

D. Aggregation driven alignment of crystals

While epitaxial match or monolayer headgroup-ion interactions may guide oriented growth during the early nucleation stages, such a mechanism cannot explain the enhanced preferential orientation at latter stages or when the number of nucleated crystals become large. Scanning electron microscopy images of samples at low and high supersaturations reveal another possibility. At low supersaturations, growth under alcohol or fatty acid monolayer consists of discrete crystals [Figs. 5(a) and 5(b)]. At higher supersaturations, however, crystals self-aggregate to form sheets consisting of linear chains of particles [Figs. 5(c) and 5(d)]. In the case of crystal growth of $\{0\ 1\ 2\}$ type crystals, the common interface

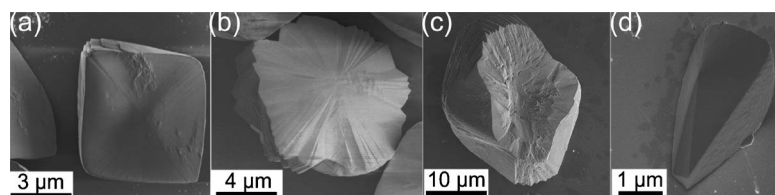


FIG. 4. Predominant morphologies observed during manganese carbonate crystal growth: [(a) and (b)] in the absence of an organic template, (c) under alcohol monolayers, and (d) under fatty acid monolayers.

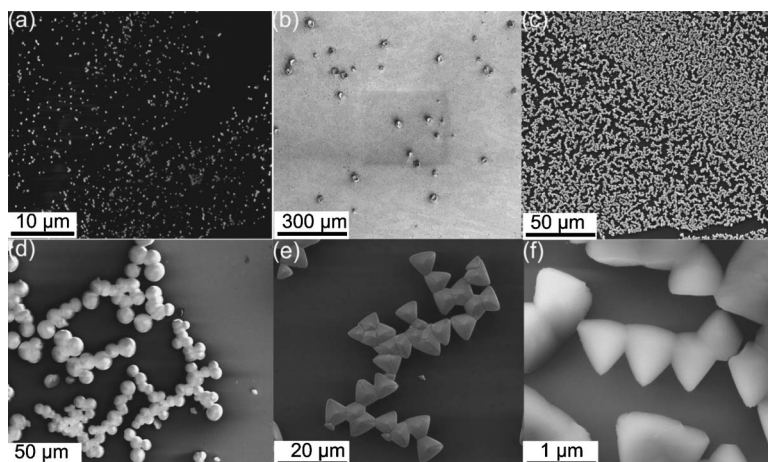


FIG. 5. Nucleation under fatty acid and alcohol monolayers: discrete crystals at low concentrations. (a) CdCO_3 crystals, grown under fatty acid monolayers, at an ionic concentration of 0.2 mM and (b) MnCO_3 crystals, grown under alcohol monolayers (concentration 2.5 mM). Crystals were collected 1 day after spreading the monolayer. CdCO_3 crystals grown under alcohol monolayers and collected after similar duration had already aggregated. The nucleation density under alcohol monolayers is much lower than that under fatty acid monolayers. At higher concentrations (within 1 h.) or even at low concentrations after longer durations (1–2 days), the nucleate under fatty acid monolayers consists of sheets of linear chains (c). GID data also show a time dependent enhanced preferred orientation for CdCO_3 crystals grown under fatty acid monolayers. We attribute this enhanced alignment to aggregation. Even crystals formed under alcohol monolayers tend to aggregate (d). Note that at higher concentrations, crystals become rounded and are smaller in size [compare Figs. 5 and 4(c)]. Linear chainlike structures of MnCO_3 crystals grown under fatty acid monolayers: 2.5 mM (after 1 day) (e) and 10 mM after 1 h. (f).

between adjoining particles either has an edge nearly parallel or perpendicular to one of the basal $\{0\ 1\ 2\}$ edges [Figs. 5(e) and 5(f)], which implies that the particles within a particular chain are perfectly oriented.

Perfect alignment and attachment of neighboring particles is a thermodynamically favorable process. The total surface energy is reduced by elimination of the neighboring interfaces and reduction in surface area of high-energy surfaces. Formation of linear chains by such a mechanism has previously been reported in titania nanoparticle growth from hydrothermally treated solutions consisting of primary titania particles.²⁹ It has also been suggested that rotation and subsequent collisions of particles, driven by random thermal motions, may align the particles and lead to the removal of adjacent crystal surfaces.⁹ However, in the case of $\{0\ 0\ 1\}$ faces nucleating under neutral alcohol monolayers, positively or negatively charged faces can face the substrate surface. In such cases, the dipole-dipole interaction of the neighboring particle may also play an important role in aligning the crystals. The $(0\ 0\ 1)$ faces are polar faces with a dipole moment perpendicular to these crystal planes. Unquenched dipole moments of neighboring particles may interact to align the crystals perfectly. Thus, Brownian motion or other short-range interactions between adjacent crystals may drive the rotation of particles.

It should also be noted that since the monolayers govern the crystal morphologies, the crystals cannot be expected to be random powders even at low concentrations; they should have some degree of preferential alignment. Thus, the rotation angles required to perfectly align the crystals are small. Further, even a slight preferential orientation, at low supersaturations, will bias the orientation during oriented attachment and enhance the alignment at the interface in that particular direction. Enhanced alignment via oriented attachment of preformed particles is the only possible explanation for our observations.

E. Degree of preferential alignment

An exact quantitative measure of the degree of preferential orientation requires complete intensity distribution along the rings. The range of our vertical scans ($K_Z \sim 0.85\ \text{\AA}^{-1}$) and hence the ring scans is limited; therefore, minimum peak intensities on the rings, i.e., the intensity contribution of the 3D powder component, cannot be easily estimated. However, absolute lower bound estimates for the fraction of crystals preferentially oriented, above the powder background, can be extracted.

We assume, for the peaks with the most symmetric intensity distribution within our scan range, that the intensity distribution along Debye rings outside our scan regions is uniform, i.e., we observe all the intensity above the 3D powder background for these peaks. The assumed 3D powder backgrounds are calculated by multiplying the absolute backgrounds measured at peak positions, in the contour scans, by a constant (Fig. 6).

The degree of preferential orientation P , within a range R of angles, around the normal is then calculated as

$$P = \frac{2 \times 3 \times \left\{ \int_R (I(\phi) - I_{3D}(\phi)) d\phi \right\}}{\left\{ 6 \times \left\{ \int_T (I(\phi) - I_{3D}(\phi)) d\phi \right\} + \left\{ \int_{180^\circ} I_{3D}(\phi) d\phi \right\} \right\}},$$

where T is the experimentally accessible scan region, I the measured peak intensities on the ring scan, and I_{3D} is the assumed 3D powder intensities. The factor of 3 arises because of the number of symmetry directions for the given set of peaks lying within half a ring, and the factor of 2 because the alignment of the crystals is only along the vertical direction, i.e., they are powders in the plane.

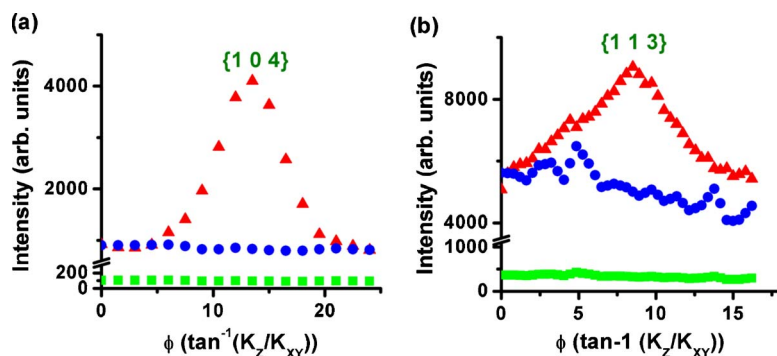


FIG. 6. Lower bound estimates for the degrees of preferred orientation: Assumed 3D powder intensities (\bullet), obtained from the observed background (\blacksquare), are subtracted from peaks with the most symmetrical intensity distributions (\blacktriangle) along “Debye” rings: (a) $\{1\ 0\ 4\}$ for CdCO_3 and (b) $\{1\ 1\ 3\}$ for MnCO_3 .

The fraction of CdCO_3 crystals preferentially oriented, at the highest supersaturation, is ~ 0.5 within $\pm 10^\circ$ of the normal, and ~ 0.3 within $\pm 3^\circ$. Similarly, for MnCO_3 the fraction of crystals within $\pm 8^\circ$ of the normal is ~ 0.2 at highest supersaturation and ~ 0.08 at the intermediate supersaturation. The range of ring scans for the MnCO_3 $\{1\ 1\ 3\}$ peaks is low ($\sim 16^\circ$), which results in overestimation of the 3D powder background and hence the low values for degree of preferred orientation. Similar, rocking curve analysis performed for crystals transferred onto silicon substrates reveals that the resulting fractions for corresponding MnCO_3 samples are higher by more than a factor of 2. From such a simplistic analysis, we can conclude that spontaneous self-aggregation can enhance the alignment of crystals, such that the degree of misorientation decreases by factors of 2 or greater.

IV. CONCLUSIONS

The morphology of CdCO_3 and MnCO_3 crystals grown from supersaturated solutions is governed by the template monolayer. The headgroup-ion interactions, rather than an epitaxial matching mechanism, govern the face selection at the interface. Although the crystals are misoriented ($> \pm 14^\circ$, about the surface normal) at lowest concentrations studied, the nucleate shows much higher preferential alignment at higher supersaturations. SEM studies of corresponding samples suggest that alignment of crystals by attachment, biased by the initial direction of crystal growth at the interface, enhances the preferential orientation.

Perfect alignment of particles from suspensions or in growth at an organic template has been reported previously,^{9,10} but the assembly of crystals observed in these studies is single-crystal-like only locally, and the average orientation of the nucleate is random. In contrast, we have observed long-range preferential alignment: 1 cm (x -ray beam width) $\times 15\text{ cm}$ (trough width).

ACKNOWLEDGMENTS

This work was supported by the U.S. Department of Energy under Grant No. DE-FG02-84ER45125. It was performed at beamline X14-A of the National Synchrotron Light Source and at beam line 1BM-C at the Advanced Photon Source. The authors thank Dr. J. Bai for his valuable assistance at the NSLS, and Dr. P. Lee for his help at the APS.

- ¹S. Mann, *Biomaterialization Principles and Concepts in Bioinorganic Materials Chemistry* (Oxford University Press, Oxford, 2001).
- ²V. M. Kaganer, H. Möhwald, and P. Dutta, *Rev. Mod. Phys.* **71**, 779 (1999).
- ³S. Mann, B. R. Heywood, S. Rajam, and J. D. Birchall, *Nature (London)* **334**, 692 (1988).
- ⁴E. V. Rakova, V. V. Klechkovskaya, N. D. Stepina, and L. A. Feigin, *Crystallogr. Rep.* **47**, S177 (2002).
- ⁵J.-M. Ouyang and S.-P. Deng, *Dalton Trans.* **14**, 2846 (2003).
- ⁶B. R. Heywood and S. Mann, *J. Am. Chem. Soc.* **114**, 4681 (1992).
- ⁷J. Kmetko, C. Yu, G. Evmenenko, S. Kewalramani, and P. Dutta, *Phys. Rev. B* **68**, 085415 (2003).
- ⁸S. Kewalramani, G. Evmenenko, C.-J. Yu, K. Kim, J. Kmetko, and P. Dutta, *Surf. Sci.* **591**, L286 (2005).
- ⁹J. F. Banfield, S. A. Welch, H. Zhang, T. T. Ebert, and R. L. Penn, *Science* **289**, 751 (2000).
- ¹⁰O. Grassmann, R. B. Neder, A. Putnis, and P. Löbmann, *Am. Mineral.* **88**, 647 (2003).
- ¹¹H. Gamsjäger, E. Könisberger, and W. Preis, *Pure Appl. Chem.* **70**, 1913 (1998).
- ¹²Determination of solubilities of metal carbonates requires precise information about ionic strengths of solutions, carbon dioxide partial pressure, $p\text{H}$, and temperature. An order of magnitude value is provided to indicate that the experiments were performed at high supersaturations.
- ¹³S. Barton, B. Thomas, E. Flom, S. Rice, B. Lin, J. Peng, J. Ketterson, and P. Dutta, *J. Chem. Phys.* **89**, 2257 (1988).
- ¹⁴M. C. Shih, M. K. Durbin, A. Malik, P. Zschack, and P. Dutta, *J. Chem. Phys.* **101**, 9131 (1994).
- ¹⁵V. Borodin, V. Lyutin, V. Ilyukhin, and N. Belov, *Dokl. Akad. Nauk SSSR* **245**, 1099 (1979).
- ¹⁶E. N. Maslen, V. A. Streltsov, N. R. Strletsova, and N. Ishizawa, *Acta Crystallogr. B.* **51**, 929 (1995).
- ¹⁷E. Busenberg and L. N. Plummer, *Geochim. Cosmochim. Acta* **49**, 713 (1985).
- ¹⁸S. Rajam and S. Mann, *J. Chem. Soc., Chem. Commun.* **24**, 1789 (1990).
- ¹⁹GID data for MnCO_3 ring scans give a better fit for $\{0\ 4\ 7\}$ crystal face parallel to the monolayer surface, i.e., the $\{0\ 1\ 2\}$ direction is $\sim 2.5^\circ$ tilted from the water surface normal. However, the rocking curves for $\{0\ 1\ 2\}$ peaks, for the corresponding samples transferred onto a solid substrate show that crystals are $\{0\ 1\ 2\}$ preferentially oriented.
- ²⁰H. Rappaport, I. Kuzmenko, M. Berfeld, K. Kjaer, J. Als-Nielsen, R. Popovitz-Biro, I. Weissbuch, M. Lahav, and L. Leiserowitz, *J. Phys. Chem. B* **104**, 1399 (2000).
- ²¹*Biomaterialization Principles and Concepts in Bioinorganic Materials Chemistry* (Ref. 1), pp. 172–173.
- ²²Two monolayer peaks are observed during the crystal growth of each metal carbonate. On supersaturated CdCO_3 subphase the peaks are observed at $K_{XY}=1.51$ and $1.68\ \text{\AA}^{-1}$ and correspond to a primitive unit cell with $a_{o1}=5\ \text{\AA}$, $b_{o1}=4.5\ \text{\AA}$, and $\gamma_{o1}=56.2^\circ$. During MnCO_3 crystal growth, the peak positions are $K_{XY}=1.505$ and $1.625\ \text{\AA}^{-1}$. The corresponding primitive unit cell parameters are $a_{o2}=4.95\ \text{\AA}$, $b_{o2}=4.59\ \text{\AA}$, and $\gamma_{o2}=57.4^\circ$. The primitive lattice parameters of the surface inorganic lattices, i.e., the $\{0\ 1\ 2\}$ crystallographic faces, are $a_c=4.95\ \text{\AA}$, $b_c=3.94\ \text{\AA}$, and $\gamma_c=51.1^\circ$, for CdCO_3 , and $a_m=4.82\ \text{\AA}$, $b_m=3.82\ \text{\AA}$, and $\gamma_m=50.9^\circ$ for MnCO_3 . The ratio of unit cell areas of the organic and the inorganic surface lattices for the two cases are very close to $\sim 5/4$ (1.23) and $\sim 4/3$ (1.33), which suggests the possibility of a geometric match at the interface. The surface lattices are related by $7a_c=a_{o1}+7b_{o1}$, $3b_c=-2a_{o1}$

+3 b_{o1} during CdCO₃ nucleation and $7a_m=4a_{o2}+4b_{o2}$, $3b_m=-1a_{o2}+3b_{o2}$ during MnCO₃ growth.

²³*Biomineralization Principles and Concepts in Bioinorganic Materials Chemistry* (Ref. 1), pp. 118–119.

²⁴J. Kmetko, A. Datta, G. Evmenenko, and P. Dutta, *J. Phys. Chem. B* **105**, 10818 (2001).

²⁵E. Loste, E. Diaz-Marti, A. Zarbaksh, and F. C. Meldrum, *Langmuir* **19**, 2830 (2003).

²⁶S. M. Hashmi, H. H. Wickman, and D. A. Weitz, *Phys. Rev. E* **72**, 041605 (2005).

²⁷A. Berman, D. J. Ahn, A. Lio, M. Salmeron, A. Reichert, and D. Charych, *Science* **269**, 515 (2005).

²⁸R. Boistelle and J. P. Astier, *J. Cryst. Growth* **90**, 14 (1988).

²⁹R. L. Penn and J. F. Banfield, *Geochim. Cosmochim. Acta* **63**, 1549 (1999).